Current Biology, Volume *32*

Supplemental Information

Inflammation and convergent placenta gene co-option contributed to a novel reproductive tissue

Leon Hilgers, Olivia Roth, Arne W. Nolte, Alina Schüller, Tobias Spanke, Jana M. Flury, Ilham V. Utama, Janine Altmüller, Daisy Wowor, Bernhard Misof, Fabian Herder, Astrid Böhne, and Julia Schwarzer

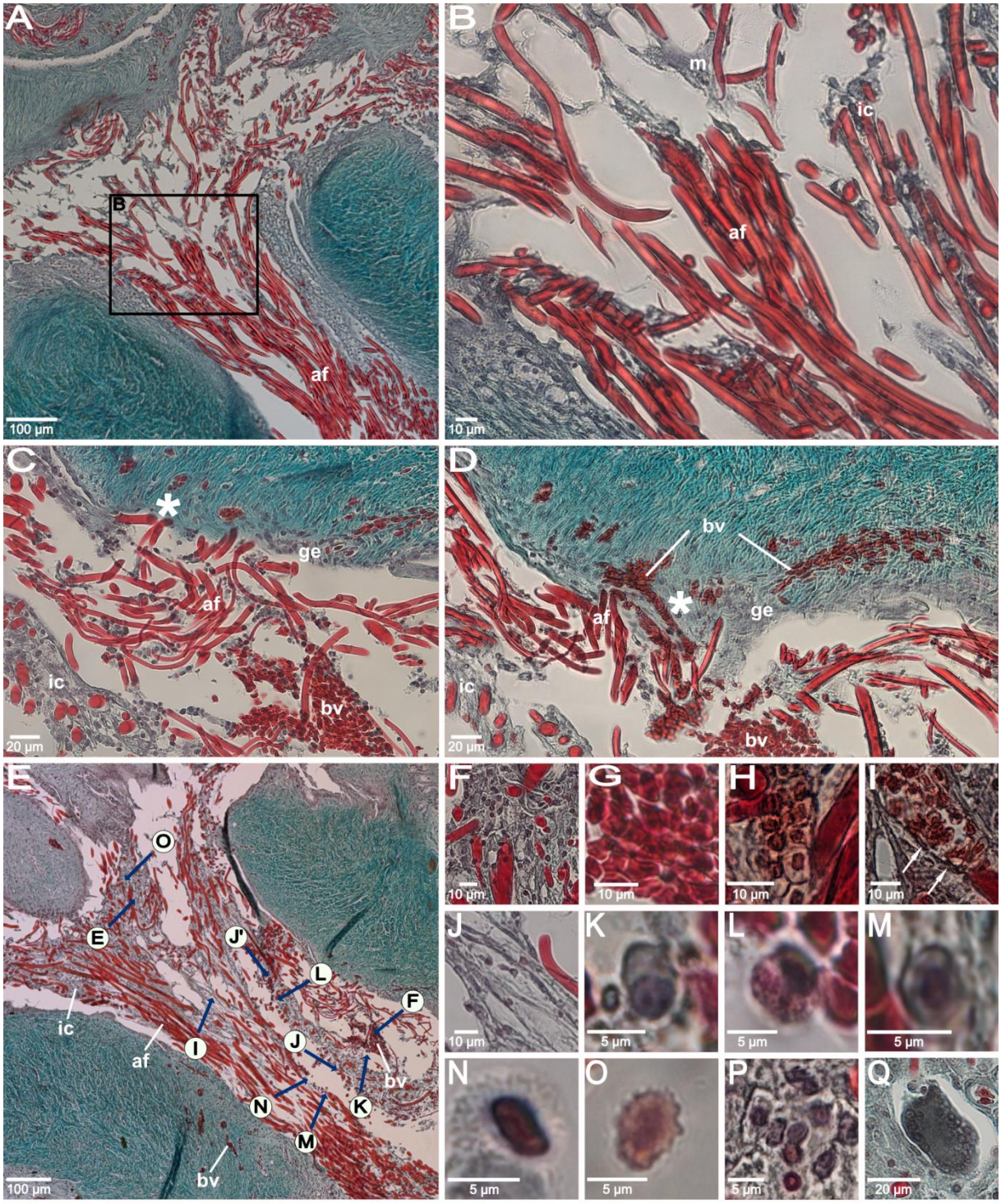

Figure S1: Micrographs of the developing plug of *O. eversi*, related to Figure 1. A) Longitudinal sections show an overview of the anterior part of the female gonoduct one day after spawning. The black square shows the location of B. B) The developing plug consisted of entangled attaching filaments (af), interstitial cells (ic) and mucus (m). Seven days after spawning, signs that attaching filaments injure the gonoduct epithelium were observed. C) Shows a site where attaching filaments (af) have breached the gonoduct epithelium (ge) (asterisk). D) Shows the same slide as in Figure 1D, but with higher

magnification. Blood vessels (bv) enter the plug at a site where attaching filaments (af) reach into a protrusion of the gonoduct epithelium (ge) (asterisk). E) At seven days after spawning, the developing plug consisted of entangled attaching filaments (af), numerous interstitial cells (ic) and blood vessels (bv). The arrows indicate the position of various cells observed in the plug. F) Round and densely colored interstitials cells with a round nucleus were located next to attaching filaments. G–H) Red-blood cells filled the blood vessels. I) Thin endothelial cells (arrows) line the blood vessels. J) Elongated, lightly colored interstitials cells with a round nucleus were located next to longer parts of attaching filaments. K) Some cells had an eccentric nuclear region, resembling plasma cells[S1] L) Granulocyte, identified based on characteristic red granules in the cytoplasm and the position of the nucleus [S1-S3]. M) Cell with a clear cell membrane and a big central nucleus. N–O) Some cells exhibited an elongated, central nucleus and an invaded cell membrane, yet the coloration differed. P) Some interstitial cells had multiple cell nuclei. These likely represent macrophages that fuse into multinucleated giant cells in the plug. Q) Sixteen days after spawning (one day after hatching) several of those multinucleated giant cells were present in the plug. Histology & staining details: Longitudinal section, trichromatic Masson–Goldner staining (light green), fixation: PFA (A–G and J–P) or Bouin Hollande (H-I and Q).

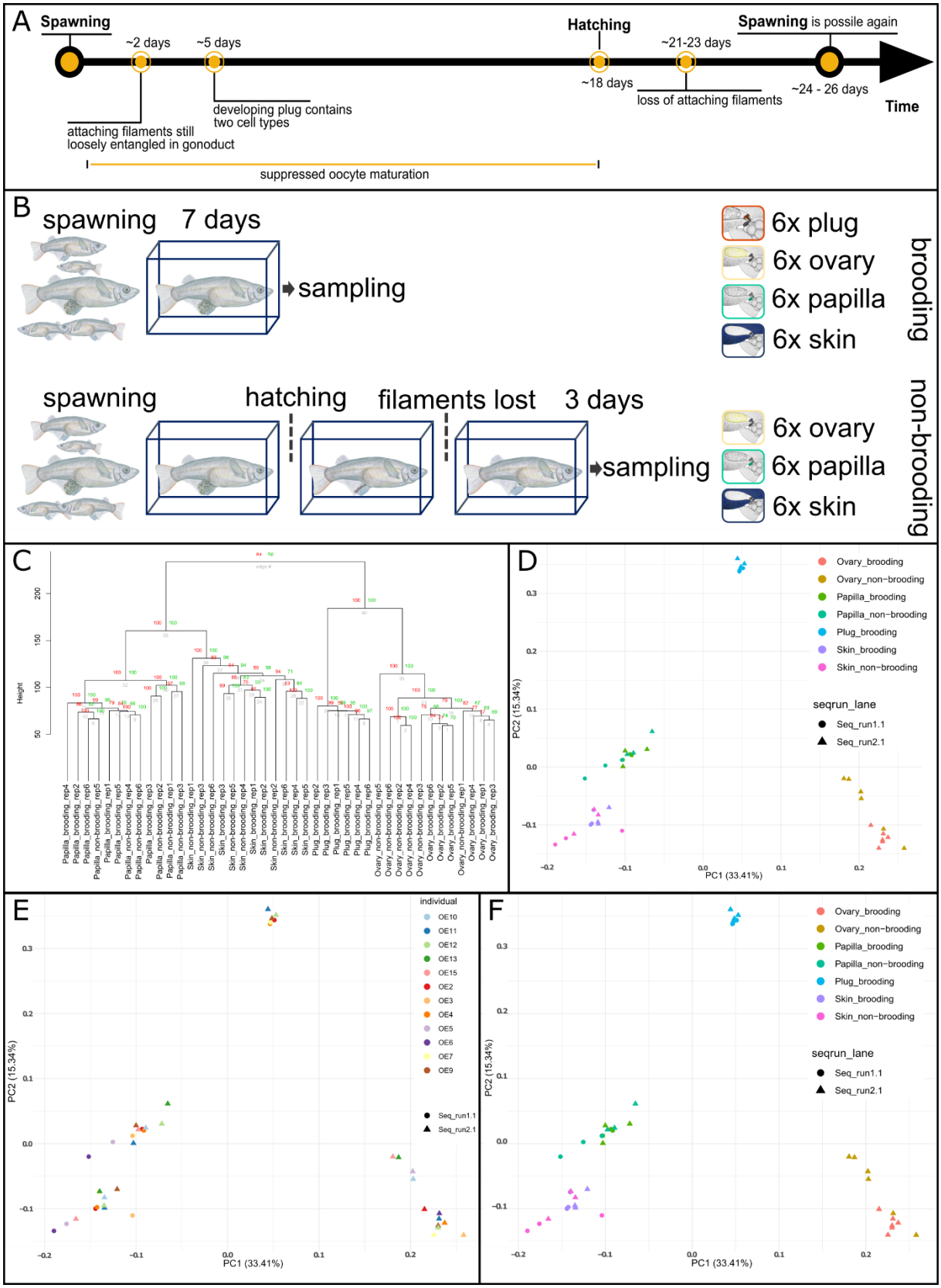

Figure S2: Overview of sampling and similarity in gene expression between samples with and without correction for batch effects, related to STAR Methods and Figure 2. A) Timeline of pelvic brooding. Illustration of an approximate timeline of pelvic brooding with key events as described for *O. sarasinorum* [S4, S5]. B) illustrates which organs were sampled at what time from brooding and non-

brooding individuals to gain insight into organ specific changes in gene expression during brooding. A total of twelve brooding females were separated and the ovary, the genital papilla, skin and the plug were harvested from six brooding females on the 7th day after oviposition. Non-brooding tissues were harvested from six females after they successfully completed their brooding cycle and could spawn again, i.e., three days after the loss of the attaching filaments. C) Support for nodes in hierarchical clustering of gene expression. Similarity in gene expression is illustrated by a hierarchical clustering tree with approximately unbiased p-value (au, red) and bootstrap probability (bp, green) for each node. Clusters comprising all samples of one tissue always have the maximal possible support (100/100). Hierarchical clustering and bootstrapping (1000x) were carried out using the R package Pvclust (45). D) Principal component analysis (PCA) of gene expression dataset. PC 1 is shown on the x-axis and PC2 on the y-axis. Colors illustrate tissue and brooding stage for each sample. Shapes indicate sequencing batches. Similar to hierarchical clustering analysis, samples of the same tissue cluster together and skin and papilla form sister clusters. Gene expression in the plug is clearly distinct. E) PCA of batch-corrected gene expression dataset. This plot is based on gene expression after batch correction for sequencing batches and tissue dissection by different experimenters. PC1 is shown on the x-axis and PC2 on the y-axis. Colors illustrate tissue and brooding stage for each sample. Shapes indicate sequencing batches. Similar to hierarchical clustering analysis, samples of the same tissue cluster together and skin and papilla form sister clusters. Gene expression in the plug is clearly distinct. General patterns remain unchanged compared to those observed without batch correction (see D for comparison). F) PCA of gene expression dataset shows sample origin by specimen. PC1 is shown on the x-axis and PC2 on the y-axis. Colors illustrate from which specimen each sample was taken. Shapes indicate sequencing batches. Samples from the same individual do not cluster, and samples of certain individuals also do not cluster consistently within tissue clusters.

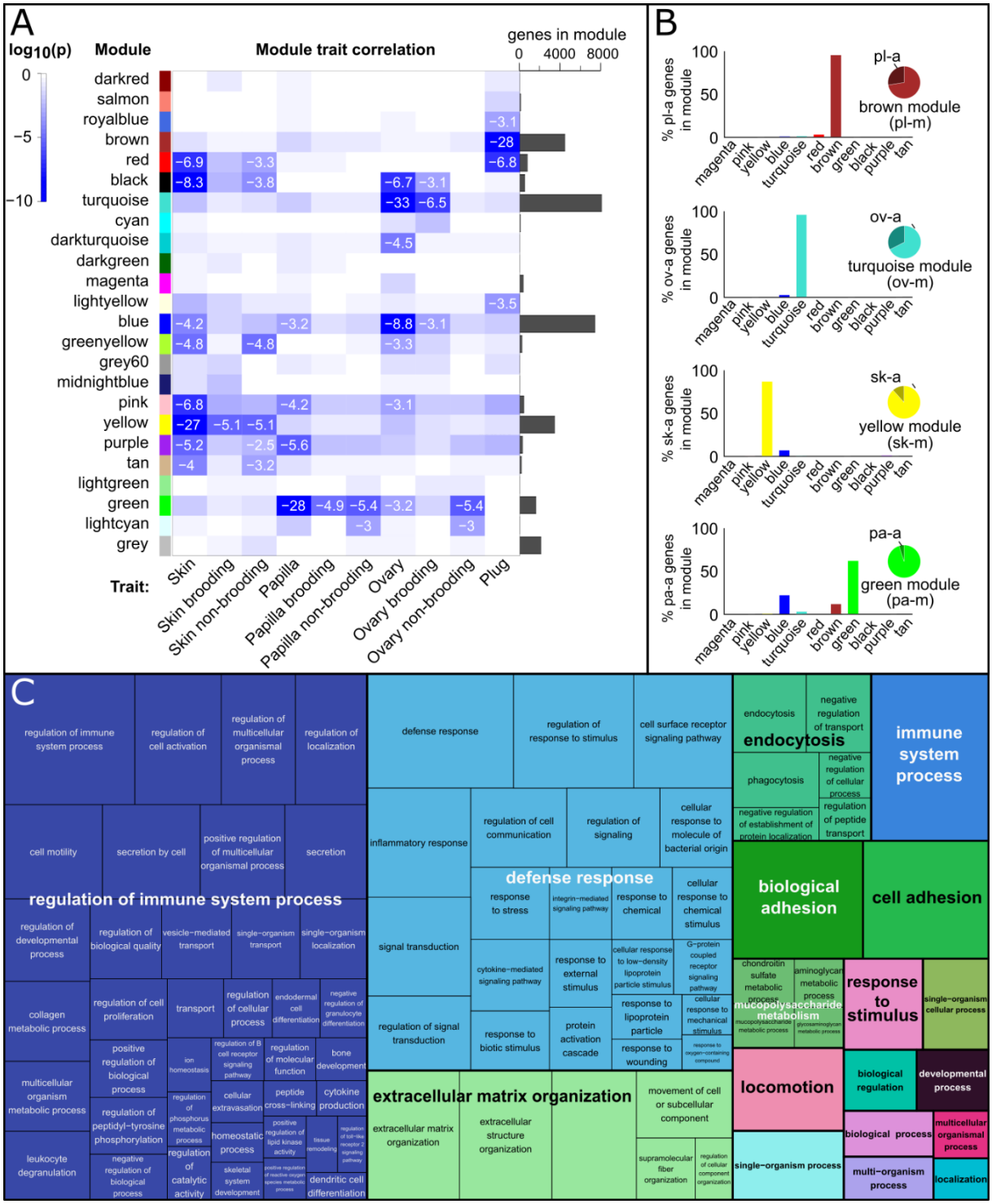

Figure S3: Organ-correlated gene sets, related to Figure 3. A) Weighted gene co-expression network analysis (WGCNA) of expressed genes across all samples. Correlation of modules (left) with each organ type in general and each organ of brooding or non-brooding individuals is illustrated with a heatmap. White and blue coloration in the heatmap indicates high and low p-values, respectively. Log10 p-values are shown for highly significant module trait correlations ($p < 0.001$). Horizontal bars (right) show the number of genes per module. The 'grey' module contains all unassigned genes. **B)** Barplots show the assignment of plug-associated (pl-a), ovary-associated (ov-a), skin-associated (sk-a) and papilla-associated (pa-a) genes into WGCNA modules. Pie charts show the proportion of tissue-associated

genes within the respective WGCNA module. **C)** Treeplot illustrates enriched biological processes (BPs) in plug-associated genes. Terms with low p-values, are indicated by large areas in the treeplot. Terms were summarized and redundant terms removed using REVIGO (Supek et al. 2011). Complete lists of all enriched gene ontologies in all organ associated gene sets and organ correlated modules are provided in Table S3.

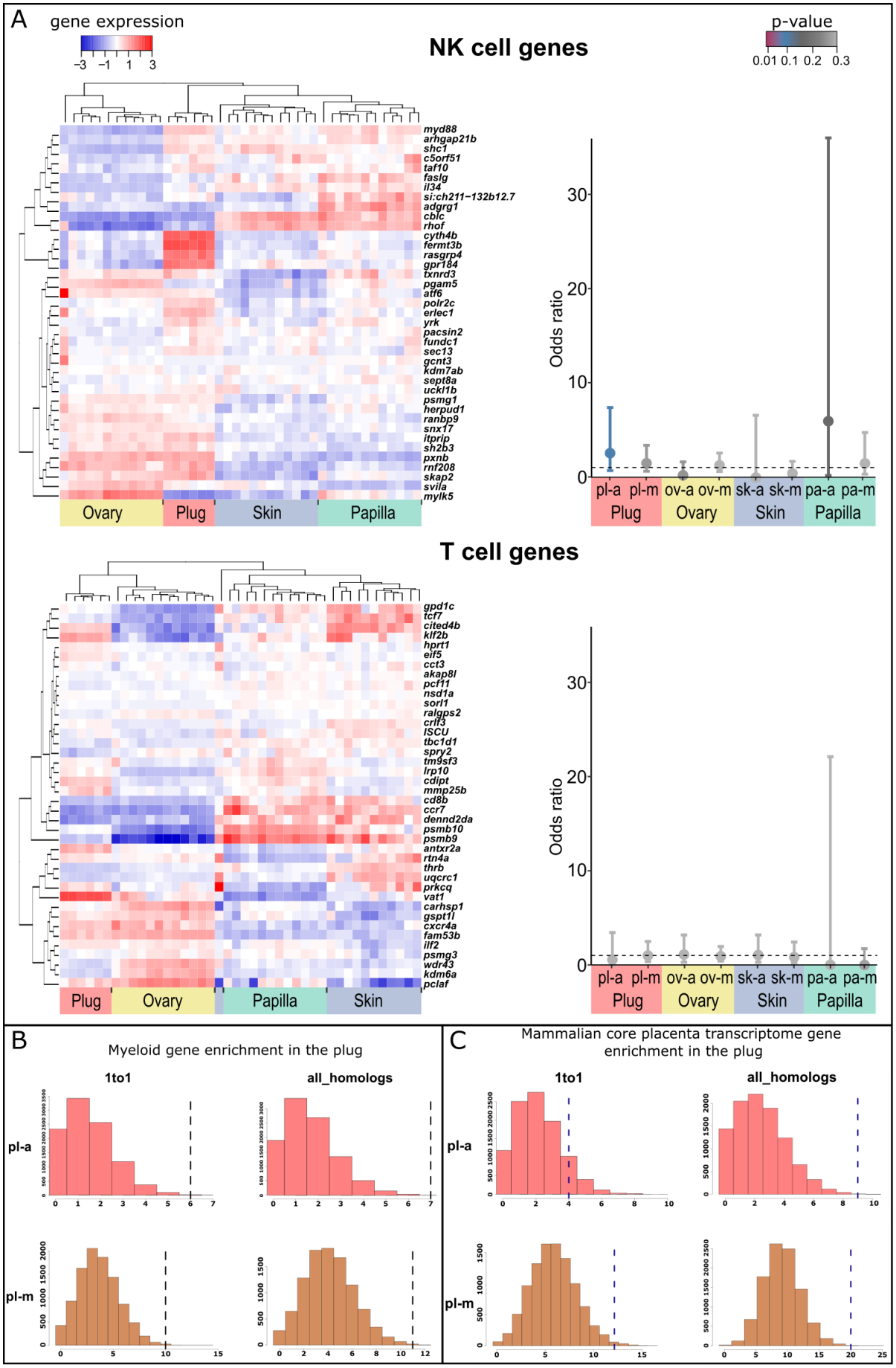
A
gene expression
−3 −1 1 3
NK cell genes
p-value
0.01 0.1 0.2 0.3
myd88
arhgap21b
shc1
c5orf51
taf10
faslg
il34
si:ch211−132b12.7
adgrg1
cblc
rhof
cyth4b
fermt3b
rasgrp4
gpr184
txnrd3
pgam5
atf6
polr2c
erlec1
yrk
pacsin2
fundc1
sec13
gcnt3
kdm7ab
sept8a
uckl1b
psmg1
herpud1
ranbp9
snx17
itprip
sh2b3
pxnb
rnf208
skap2
svila
mylk5
Ovary
Plug
Skin
Papilla
Odds ratio
0
10
20
30
pl-a
pl-m
ov-a
ov-m
sk-a
sk-m
pa-a
pa-m
Plug
Ovary
Skin
Papilla
T cell genes
gpd1c
tcf7
cited4b
klf2b
hprt1
eif5
cct3
akap8l
pcf11
nsd1a
sorl1
ralgps2
crlf3
ISCU
tbc1d1
spry2
tm9sf3
lrp10
cdipt
mmp25b
cd8b
ccr7
dennd2da
psmb10
psmb9
antxr2a
rtn4a
thrb
uqcrc1
prkcq
vat1
carhsp1
gspt1l
cxcr4a
fam53b
iif2
psmg3
wdr43
kdm6a
pclaf
Plug
Ovary
Papilla
Skin
Odds ratio
0
10
20
30
pl-a
pl-m
ov-a
ov-m
sk-a
sk-m
pa-a
pa-m
Plug
Ovary
Skin
Papilla
B
Myeloid gene enrichment in the plug
1to1
all_homologs
pl-a
pl-m
C
Mammalian core placenta transcriptome gene enrichment in the plug
1to1
all_homologs
pl-a
pl-m

Figure S4: Expression and enrichment of immune cell marker genes and mammalian core placenta transcriptome genes, related to Figure 3 and Figure 4. A) Expression of NK and T cell genes in *O. eversi*. The left side shows centered log2 transformed gene expression of NK cell- (n = 39) and T cell- (n = 40) marker genes. Genes are represented as horizontal bars across samples (columns). Over-expression is shown in red while under-expression is shown in blue in the heatmap. Similarity in gene expression between samples is shown with the hierarchical clustering tree on the top, while similarity in expression between genes is shown in the hierarchical clustering tree on the left. On the right side, frequency of immune cell genes compared to the entire transcriptome is shown as odds ratio for tissue-associated gene sets (-a) and tissue-correlated WGCNA modules (-m). Whiskers show 95% confidence intervals and color indicates whether odds ratios are significantly different from one, i.e., whether immune cell genes are significantly more or less frequent in a gene set than would be expected by chance using a Fisher's exact test. **B)** Likelihood of observed myeloid cell marker enrichment in the plug. Histograms show distribution of expected overlaps between human genes and the pl-a gene set (top, red) or the pl-m (bottom, brown). Distributions are based on 10,000 randomly sampled datasets of human genes with 1:1_orthologs (28 genes, left) or any homolog (31 genes, right) in our transcriptome. Dotted lines show the observed overlap with genes of the mammalian core placenta transcriptome, which was significantly increased for pl-a genes (all homologs) and the pl-m (1to1 and all homologs). **C)** Likelihood of observed mammalian core placenta transcriptome enrichment in the plug. Histograms show distribution of expected overlaps between human genes and the pl-a gene set (top, red) or the pl-m (bottom, brown). Distributions are based on 10,000 randomly sampled datasets of human genes with 1:1_orthologs (41 genes, left) or any homolog (59 genes, right) in our transcriptome. Dotted lines show the observed overlap with genes of the mammalian core placenta transcriptome, which was significantly increased for pl-a genes (all homologs) and the pl-m (1to1 and all homologs).

Table S1. Assembly statistics of the raw and filtered assembly, related to STAR Methods

	Trinity genes	GC (in %)	'gene' N50	Complete[a] (in %)	Duplicated[a] (in %)
Raw assembly	66 967	47.4	2 504	82.9	2.4
Filtered assembly	30 643	47.3	3 008	85.4	2.1

[a] According to BUSCO

Supplemental References

S1. V. Blüm, J. Casado, J. Lehmann, E. Mehring, "Grundlagen der Makroskopischen Anatomie der Regenbogenforelle" in *Farbatlas Der Histologie Der Regenbogenforelle*, (Springer Berlin Heidelberg, 1989), pp. 2–8.

S2. D. M. Mokhtar, E. A. Abdelhafez, An overview of the structural and functional aspects of immune cells in teleosts. *Histol. Histopathol.* **36**, 399–414 (2021).

S3. J. Boomker, The haematology and histology of the haemopoietic organs of South African freshwater fish. III. The leucocytes, plasma cells and macrophages of Clarias gariepinus and Sarotherodon mossambicus. *Onderstepoort J. Vet. Res.* **48**, 185–93 (1981).

S4. T. Iwamatsu, H. Kobayashi, M. Sato, M. Yamashita, Reproductive role of attaching filaments on the egg envelope in Xenopoecilus sarasinorum (Adrianichthidae, Teleostei). *J. Morphol.* **269**, 745–750 (2008).

S5. T. Iwamatsu, *et al.*, Oviposition cycle in the oviparous fish Xenopoecilus sarasinorum. *Zoolog. Sci.* **24**, 1122–1127 (2007).